

Anterior Cruciate Ligament Loading Increases With Pivot-Shift Mechanism During Asymmetrical Drop Vertical Jump in Female Athletes

Ryo Ueno,^{*†‡} PT, PhD, Alessandro Navacchia,^{†§} PhD, Nathan D. Schilaty,^{†||¶} DC, PhD, Gregory D. Myer,^{#**††} PhD, Timothy E. Hewett,^{††§§} PhD, and Nathaniel A. Bates,^{†||} PhD

Investigation performed at the Mayo Clinic, Rochester, Minnesota, USA

Background: Frontal plane trunk lean with a side-to-side difference in lower extremity kinematics during landing increases unilateral knee abduction moment and consequently anterior cruciate ligament (ACL) injury risk. However, the biomechanical features of landing with higher ACL loading are still unknown. Validated musculoskeletal modeling offers the potential to quantify ACL strain and force during a landing task.

Purpose: To investigate ACL loading during a landing and assess the association between ACL loading and biomechanical factors of individual landing strategies.

Study Design: Descriptive laboratory study.

Methods: Thirteen young female athletes performed drop vertical jump trials, and their movements were recorded with 3-dimensional motion capture. Electromyography-informed optimization was performed to estimate lower limb muscle forces with an OpenSim musculoskeletal model. A whole-body musculoskeletal finite element model was developed. The joint motion and muscle forces obtained from the OpenSim simulations were applied to the musculoskeletal finite element model to estimate ACL loading during participants' simulated landings with physiologic knee mechanics. Kinematic, muscle force, and ground-reaction force waveforms associated with high ACL strain trials were reconstructed via principal component analysis and logistic regression analysis, which were used to predict trials with high ACL strain.

Results: The median (interquartile range) values of peak ACL strain and force during the drop vertical jump were 3.3% (–1.9% to 5.1%) and 195.1 N (53.9 to 336.9 N), respectively. Four principal components significantly predicted high ACL strain trials, with 100% sensitivity, 78% specificity, and an area of 0.91 under the receiver operating characteristic curve ($P < .001$). High ACL strain trials were associated with (1) knee motions that included larger knee abduction, internal tibial rotation, and anterior tibial translation and (2) motion that included greater vertical and lateral ground-reaction forces, lower gluteus medius force, larger lateral pelvic tilt, and increased hip adduction.

Conclusion: ACL loads were higher with a pivot-shift mechanism during a simulated landing with asymmetry in the frontal plane. Specifically, knee abduction can create compression on the posterior slope of the lateral tibial plateau, which induces anterior tibial translation and internal tibial rotation.

Clinical Relevance: Athletes are encouraged to perform interventional and preventive training to improve symmetry during landing.

Keywords: ACL; finite element; knee; landing; strain

Anterior cruciate ligament (ACL) injuries are one of the most devastating injuries in sports. While surgical reconstruction is the clinical standard of care for a ruptured ACL, problems that persist after the reconstruction include a lengthy rehabilitation, a low rate of return to sports, and

a high rate of reinjury of the graft.^{1,17,43} Injury reduction remains the most effective way to resolve these circumstances, and it is therefore important to study injury mechanisms to develop effective reduction programs.²¹ Landing is the most frequent athletic motor task associated with ACL injuries.⁷ Accordingly, cadaveric simulations of landing tasks were developed and have revealed that externally applied knee abduction moment, anterior tibial force, internal tibial rotation moment, and impulsive

The Orthopaedic Journal of Sports Medicine, 9(3), 2325967121989095
DOI: 10.1177/2325967121989095
© The Author(s) 2021

This open-access article is published and distributed under the Creative Commons Attribution - NonCommercial - No Derivatives License (<https://creativecommons.org/licenses/by-nc-nd/4.0/>), which permits the noncommercial use, distribution, and reproduction of the article in any medium, provided the original author and source are credited. You may not alter, transform, or build upon this article without the permission of the Author(s). For article reuse guidelines, please visit SAGE's website at <http://www.sagepub.com/journals-permissions>.

ground-reaction forces induce ACL strain and rupture.^{2,4,5,46,47,50} Although these in vitro simulations aimed to simulate joint loading during in vivo landing, there remains a gap in knowledge relative to the complex nature of individual landing strategies, inclusive of patient-specific kinematics and muscle activations.

While ACL strain is influenced by multiplane loading,^{14,29,33} knee abduction moment during landing is a predictor of ACL injury, and it increases ACL strain in cadaveric simulations.^{2-5,25,46,47,50} A recent musculoskeletal modeling study demonstrated that knee abduction moment was larger during landing in the frontal plane, with higher vertical and lateral ground-reaction force, lower gluteus medius force, and a laterally shifted and tilted pelvic position.⁵¹ This musculoskeletal modeling study⁵¹ supported a previously proposed ACL injury mechanism in frontal plane mechanics.²⁴

Three-dimensional motion capture systems and musculoskeletal modeling have been used to investigate in vivo biomechanics and neuromuscular activations and forces during landing tasks.^{32,36,37,41,49,51} With the advance of musculoskeletal modeling and its optimization techniques, the estimation of muscle activations and forces better captures muscle physiology as compared with classic static optimization methods.^{19,45} However, only a few musculoskeletal modeling studies have reported ligament loading and knee joint contact force with validated material properties and a 6 degrees of freedom (DOF) knee joint, which is necessary to obtain accurate ligament loading.

A validated specimen-specific musculoskeletal finite element (FE) model has the potential to address these limitations, as it could reveal the precise 6 DOF knee kinematics in response to observed muscle forces and ground-reaction forces.^{26,27,40} Thus, associations between ACL load and whole-body biomechanics during landing can be evaluated with a validated musculoskeletal FE model.

The purpose of this study was to assess the association between ACL loading calculated in a validated FE model and biomechanical factors of individual landing strategies measured in vivo during landing. In this article, landings where there is a frontal plane trunk lean with a side-to-side difference in lower extremity biomechanics are referred to

as *asymmetrical*. The hypothesis was that a simulated landing with asymmetry in the frontal plane would show higher ACL strain and force as compared with a symmetric landing. Specifically, it was hypothesized that the trials with higher estimated ACL strain and force would be associated with higher vertical and lateral ground-reaction forces, lower gluteus medius force, and laterally shifted and tilted pelvic motion, as reported in previous studies.^{24,51} This information will contribute to the understanding of ACL biomechanics during in vivo landings and to the development of injury screening and reduction protocols.

METHODS

Experimental Testing

Thirteen young female athletes participated in this study (mean \pm SD age, 15.6 \pm 1.6 years; height, 169.8 \pm 5.6 cm; mass, 62.6 \pm 5.2 kg). Each participant performed 3 drop vertical jump (DVJ) trials. The participants were instructed to drop from a 30 cm-high box onto 2 force plates (AMTI) and to immediately perform a maximum vertical jump. Institutional review board approval and informed consent were obtained before the execution of this study.

A total of 35 reflective markers were placed on the athlete, and marker trajectories were collected using a motion capture system (EVA-RT Version 5; Motion Analysis Corp) with 10 digital cameras (Eagle cameras; Motion Analysis Corp) sampled at 240 Hz. Ground-reaction forces were synchronously recorded at 1200 Hz with the 2 force plates. Kinematic and ground-reaction force data were low-pass filtered using a zero-lag fourth-order Butterworth filter at 12 and 50 Hz, respectively.⁵¹ Surface electromyography (EMG) data for the right leg were measured using a telemetry surface EMG system (TeleMyo 2400; Noraxon) at a sampling rate of 1200 Hz. The electrodes were placed on the biceps femoris, semitendinosus, rectus femoris, vastus lateralis, vastus medialis, gastrocnemius medialis, adductor longus (to represent the adductor longus and gracilis during muscle force estimation), and gluteus medius of each participant.^{8,11,15} The raw EMG data were band-pass filtered, full-wave rectified, and low-pass filtered at 6 Hz.⁵¹

*Address correspondence to Ryo Ueno, PT, PhD, Department of Sport Science, University of Innsbruck, Fürstenweg 185, A-6020 Innsbruck, Austria (email: ryo.ueno@uibk.ac.at).

[†]Department of Orthopedic Surgery, Mayo Clinic, Rochester, Minnesota, USA.

[‡]Department of Sport Science, University of Innsbruck, Innsbruck, Austria.

[§]Smith & Nephew, San Clemente, California, USA.

^{||}Department of Physiology and Biomedical Engineering, Mayo Clinic, Rochester, Minnesota, USA.

[¶]Department of Physical Medicine and Rehabilitation, Mayo Clinic, Rochester, Minnesota, USA.

[#]The SPORT Center, Division of Sports Medicine, Cincinnati Children's Hospital Medical Center, Cincinnati, Ohio, USA.

^{**}Departments of Pediatrics and Orthopedic Surgery, College of Medicine, University of Cincinnati, Cincinnati, Ohio, USA.

^{††}The Micheli Center for Sports Injury Prevention, Waltham, Massachusetts, USA.

^{‡‡}Hewlett Global Consulting, Rochester Minnesota, USA.

^{§§}The Rocky Mountain Consortium for Sports Research, Edwards, Colorado, USA.

Final revision submitted September 30, 2020; accepted October 28, 2020.

One or more of the authors has declared the following potential conflict of interest or source of funding: The authors acknowledge funding from the National Institutes of Health (grants R01AR049735, R01AR056259, R01AR055563, K12HD065987, and L30AR070273). A.N. is an employee of Smith & Nephew. G.D.M. has received royalties from Human Kinetics and Wolters Kluwer and has a patent pending. AOSSM checks author disclosures against the Open Payments Database (OPD). AOSSM has not conducted an independent investigation on the OPD and disclaims any liability or responsibility relating thereto.

Ethical approval for this study was obtained from Cincinnati Children's Hospital Medical Center (study 2008-0023).

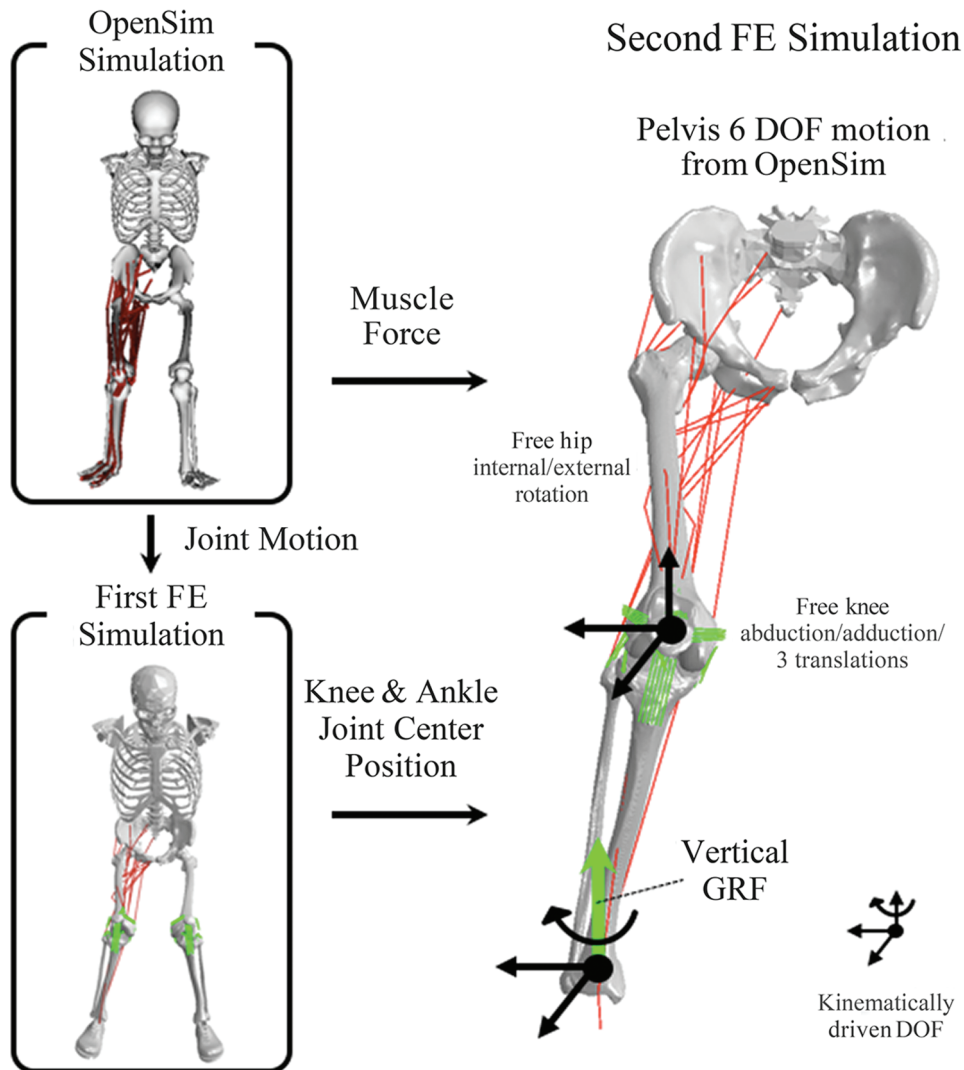


Figure 1. Work flow of the computational modeling to estimate ligament loading during the drop vertical jump, in which individual landing strategies were maintained. Joint motion and muscle forces were estimated using electromyography-informed optimization in OpenSim simulation. Joint motion was inputted to first finite element (FE) simulation to simulate the same landing and obtain nodal coordinates of knee and ankle joint center positions. To simulate more physiologic knee joint mechanics, the joint center position was kinematically driven, and muscle forces from OpenSim simulation were applied in the second FE simulation. Black arrows on the joint center indicate kinematically driven degrees of freedom (DOF). Inferosuperior DOF on the ankle joint were unconstrained to apply vertical ground-reaction force (GRF), whereas rotation on the transverse plane was kinematically driven to track toe direction. The pelvis was kinematically driven with 6 DOF motion according to OpenSim simulation. This allows hip internal/external rotation as well as knee abduction/adduction and 3 DOF translations to be unconstrained and dependent on muscle force, joint contact force, and GRF for physiologic simulation.

Processed EMG data were normalized to peak EMG magnitudes from the athlete across all the motor activities performed during data collection, which included open chain maximum voluntary contractions and DVJ from different drop heights (15 and 45 cm).³⁴

Computational Simulations

To estimate ACL strain and force during landings, sequential OpenSim simulations and FE simulations were executed. Joint motions and muscle forces were estimated in

the OpenSim simulations and inputted to FE simulations to estimate ACL strain and force in a response to the joint motion, muscle forces, and ground-reaction force (Figure 1).

OpenSim Simulations. Muscle forces were estimated with OpenSim 3.3 as previously described.⁵¹ Briefly, a generic musculoskeletal model⁴⁴ with additional DOF of knee abduction/adduction and internal/external rotation and additional hip external rotator muscles was scaled to the participant's body size and weight. The maximum isometric force of each muscle was increased by 20% to enable the muscles to generate the required joint torques during

landing. The scaled models were used to obtain the joint kinematics and muscle forces using EMG-informed direct collocation in OpenSim and custom MATLAB code (R2017b; MathWorks). An objective function was aimed to track patient-specific measured EMG signals. In the musculoskeletal modeling step, 2 trials did not achieve the tolerance of muscle force optimization and were excluded from the analysis.

FE Simulations. One of 4 previously developed and validated specimen-specific FE models of the knee (from specimen “ML” [male, left leg], see Navacchia et al³⁹) was utilized to create a musculoskeletal FE model in this study. Briefly, the previously validated FE model of the knee included specimen-specific bone and cartilage geometries and calibrated ligaments on the tibiofemoral and patellofemoral joint.³⁹ The material properties of the ligaments, including stiffness and reference strain, were computationally optimized to match measurements from in vitro experimental testing by minimizing the results from model and experiments. The in vitro experimental testing included kinematic and ACL strain measurements under a variety of external loading conditions, which included anterior tibial shear force, knee abduction moment, internal tibial rotation moment, and ground-reaction force. The experimental measurements were performed at 25° of knee flexion.

In the present study, a generic model of the pelvis was added to the knee model using ABAQUS/Explicit (SIMULIA). The subsequent musculoskeletal FE model included a 3 DOF ball joint at the hip, 12 DOF knee joint (6 DOF tibiofemoral and 6 DOF patellofemoral),³⁹ and 1 DOF hinge joint at the ankle. A total of 24 muscles that span the hip and knee joints were modeled as unidimensional connectors, consistent with the OpenSim simulations.

The same landing tasks simulated with OpenSim were also simulated with the FE model. Individual landing strategies (eg, knee-in, toe-out) were maintained, as determined by the knee and ankle joint center location and toe direction. First, pelvic, hip, knee, and ankle joints were kinematically driven on the basis of the joint angles obtained from the OpenSim simulation inverse kinematics, and the positions in space of the knee joint center (midpoint between medial and lateral knee condyles) and ankle joint center (midpoint between medial and lateral malleoli) during landing were recorded. In the second FE simulation, the knee and ankle joint center positions were driven kinematically according to the first step, and the rotational and translational DOF on the hip and knee joints remained unconstrained. The muscle forces and the vertical ground-reaction force were applied to each muscle and to the ankle, respectively. The mediolateral and anteroposterior positions of the ankle joint center were also driven, while the inferosuperior position was left free to transfer correctly the ground force to the knee. In addition, a point on the ankle located 10 mm in front of the ankle joint center was kinematically driven in the mediolateral position to track the toe direction during landing.

This strategy was performed to simulate the physiological knee joint mechanics, in which internal/external hip rotation and knee abduction/adduction and translational

DOF depend on muscle, ligament, contact, and ground-reaction forces, while maintaining the individual landing strategies. Only the vertical component of ground-reaction force was applied at the ankle joint center because all the other DOF (anteroposterior and mediolateral translation and the rotation on transverse plane) were kinematically driven (Figure 1).

ACL strain and force were averaged and summed, respectively, across the 4 modeled fibers (2 fibers each in the anteromedial and posterolateral bundles of the ACL). ACL strain was calculated as $100 \times (L - L_0)/L_0$, where L and L_0 are current length and reference length (slack length determined by optimization in validation step³⁹), respectively. L_0 values for the anteromedial and posterolateral bundles of the ACL were 33.4 and 17.6 mm, respectively, and the same value was used for both fibers in a bundle. The resultant kinematics of the hip and knee joint were extracted from the FE simulation. The knee joint kinematics were calculated according to the coordinate system of Grood and Suntay.¹⁸ The OpenSim simulation results were used for the outcomes of pelvic and trunk kinematics and muscle forces.

Statistical Analysis

The third quartiles of ACL strain/force were calculated and set as thresholds to define high-strain/force trials. To identify which variables and which time range predicted the occurrence of high ACL strain during landing, a principal component (PC) analysis was performed with the kinematic, ground-reaction force, and muscle force continuous data, as described in a previous study.⁵⁰ All data were trimmed from initial contact (IC) to 100 milliseconds after IC and resampled to 101 data points. This time range was selected to focus on the period where maximal ACL strain and ACL rupture events occurred during previous cadaveric simulations.^{6,30,50} PC analysis was performed after the data were standardized to a z score. In total, 36 PCs were assessed with the broken stick method, which detects the significant PCs that explain the variance more than PCs derived from a random data set.²⁸ With this method, the first 7 PCs were detected as significant and were incorporated in the logistic regression.

Logistic regression analyses were performed to choose the PCs that predicted high ACL strain trials. The best-fit model was selected with the forward direction stepwise minimum Bayesian information criterion. Sensitivity, specificity, and area under the receiver operator characteristic curve were used to assess how well the logistic regression analysis predicted the occurrence of high ACL strain trials and high ACL force trials. Waveforms that presented features of high ACL strain trials were reconstructed using the PCs selected by logistic regression. The low- and high-risk waveforms were reconstructed on each variable. PC analysis and the corresponding data processing were performed using custom MATLAB code, while the logistic regression analysis was performed with JMP (Version 14 Pro; SAS Institute Inc). Statistical significance was set to $P < .05$.

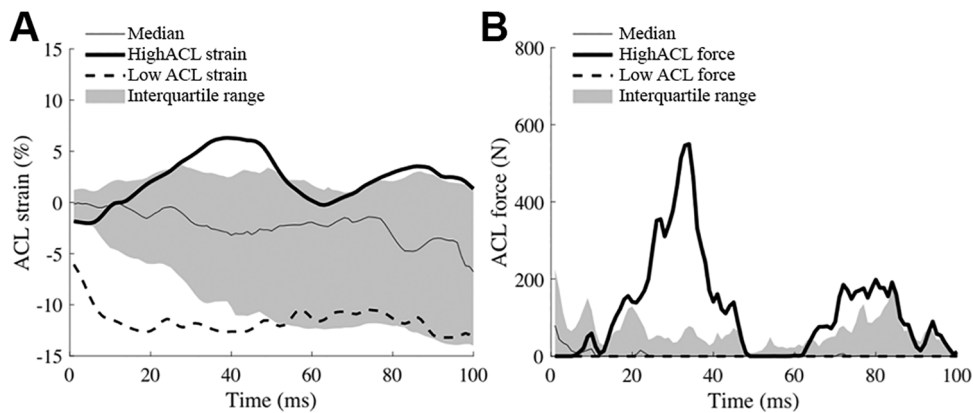


Figure 2. Median, interquartile range, and representative trials of (A) high and low ACL strain and (B) ACL force. Time zero indicates time of the initial contact to the ground. ACL, anterior cruciate ligament.

RESULTS

Median (interquartile range) peak ACL strain and force during landing were 3.3% (−1.9% to 5.1%) and 195.1 N (53.9 to 336.9 N), respectively (Figure 2). The third quartiles of the ACL strain, 5.1% was chosen as the cutoff value to detect high ACL strain trials. The median (interquartile range) time of peak ACL strain and force within the trials with more than the third quartile of strain or force were 56 milliseconds (29.5–100 milliseconds) and 34 milliseconds (8–84 milliseconds), respectively.

Trials with high ACL strain were significantly predicted by 4 PCs in the logistic regression ($P < .001$). The logistic regression model presented 100% sensitivity, 78% specificity, and an area of 0.91 under the receiver operator characteristic curve (Figure 3). The PCs that predicted high ACL strain trials were high PC2 score, low PC4 score, low PC6 score, and high PC7 score.

High-risk waveforms were reconstructed using the 4 PCs included in the logistic regression model and demonstrated the features of high ACL strain trials. With regard to knee joint kinematics, knee abduction, internal tibial rotation, and tibial translation in the anterior, medial, and superior directions were higher in the high-risk waveforms compared with the low-risk waveforms from IC to 100 milliseconds after IC (Figure 4).

The high-risk waveforms showed larger peak ground-reaction forces (vertical: at approximately 75 milliseconds; lateral: immediately after IC), as well as lower gluteus medius force from IC to 100 milliseconds after IC. Furthermore, larger lateral pelvic tilt and hip adduction (indicative of lateral pelvic shift⁵¹) from IC to 100 milliseconds after IC were observed (Figure 5). The muscle forces were mostly lower in the high-risk waveforms except for the iliopsoas, vastus intermedius, and gastrocnemius medialis. The waveforms for all muscle forces are available in the Appendix.

DISCUSSION

This study was conducted to analyze the relationship between estimated ACL loading and biomechanical

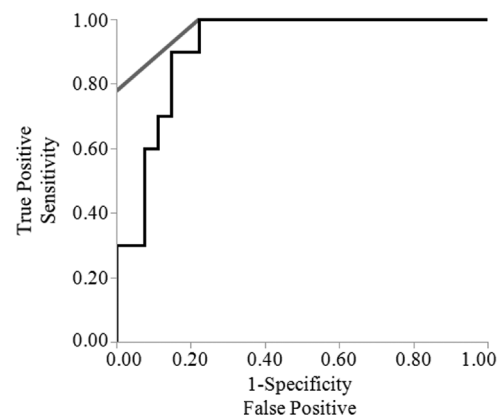


Figure 3. ROC curve of the 4 principal components that predicted high anterior cruciate ligament strain trials with 100% sensitivity, 78% specificity, and an area of 0.91 under the ROC curve. ROC, receiver operating characteristic.

variables during a variety of simulated DVJ trials. The assessment of ACL loading was performed with a whole-body musculoskeletal FE model. This was the first study to estimate absolute ACL strain and force during an in vivo landing using a specimen-specific, validated FE model. The hypothesis was that ACL loading would be higher in asymmetrical landing in the frontal plane, especially with (1) higher vertical and lateral ground-reaction forces, (2) lower gluteus medius force, and (3) laterally tilted and shifted pelvic motion. The hypothesis was investigated using reconstructed waveforms from PCs that predicted the trials with high ACL strain in a logistic regression model. Our hypothesis was supported, as the peak vertical and lateral ground-reaction force was higher, the gluteus medius force was lower, and the lateral pelvic tilt and hip adduction (indicative of lateral pelvic shift⁵¹) were higher in the high-risk waveforms. Therefore, this study demonstrated that estimated ACL loading was greater during simulations of the participants' landings that exhibited asymmetry in the frontal plane than in landings that were symmetrical.

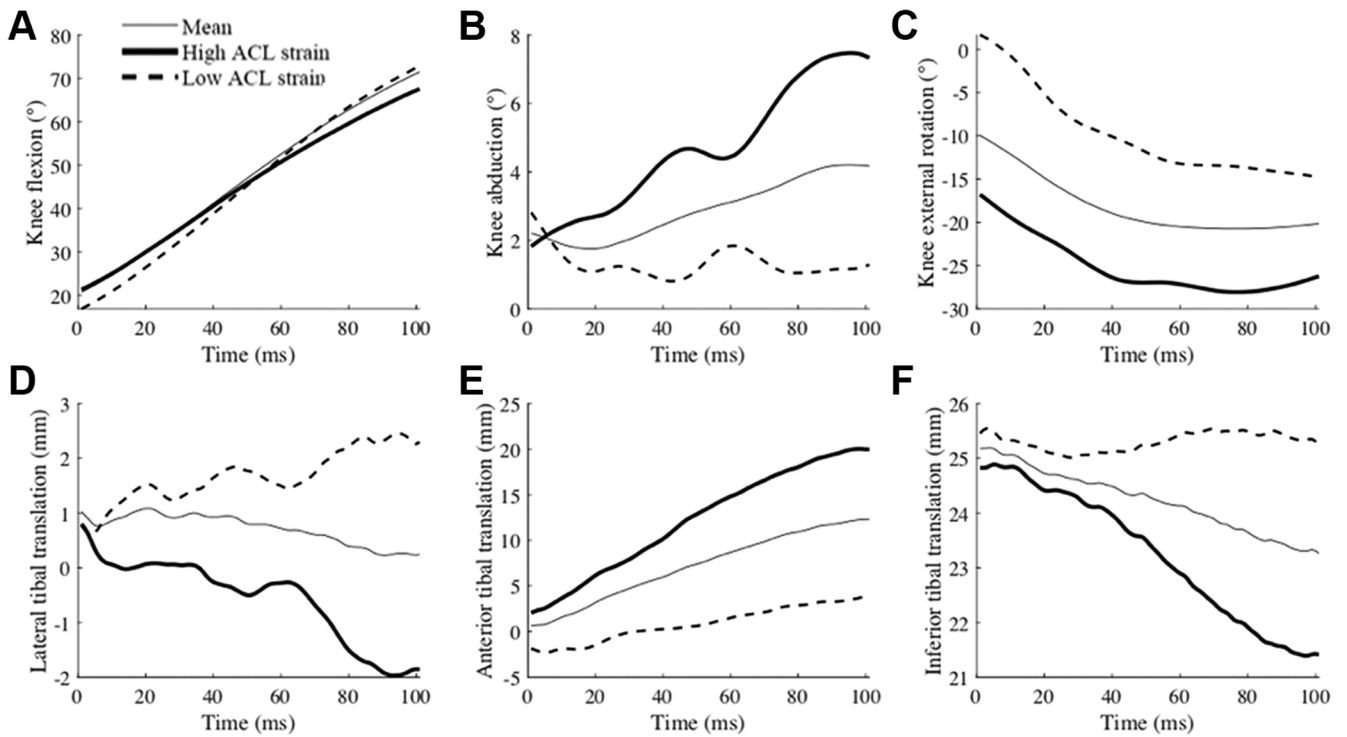


Figure 4. Mean (thin), high ACL strain (thick), and low ACL strain (dashed) waveforms of (A) knee flexion, (B) knee abduction, (C) knee external rotation, (D) lateral tibial translation, (E) anterior tibial translation, and (F) inferior tibial translation reconstructed from the 4 principal components that significantly predicted high ACL strain trials. Time zero indicates initial contact to the ground. ACL, anterior cruciate ligament.

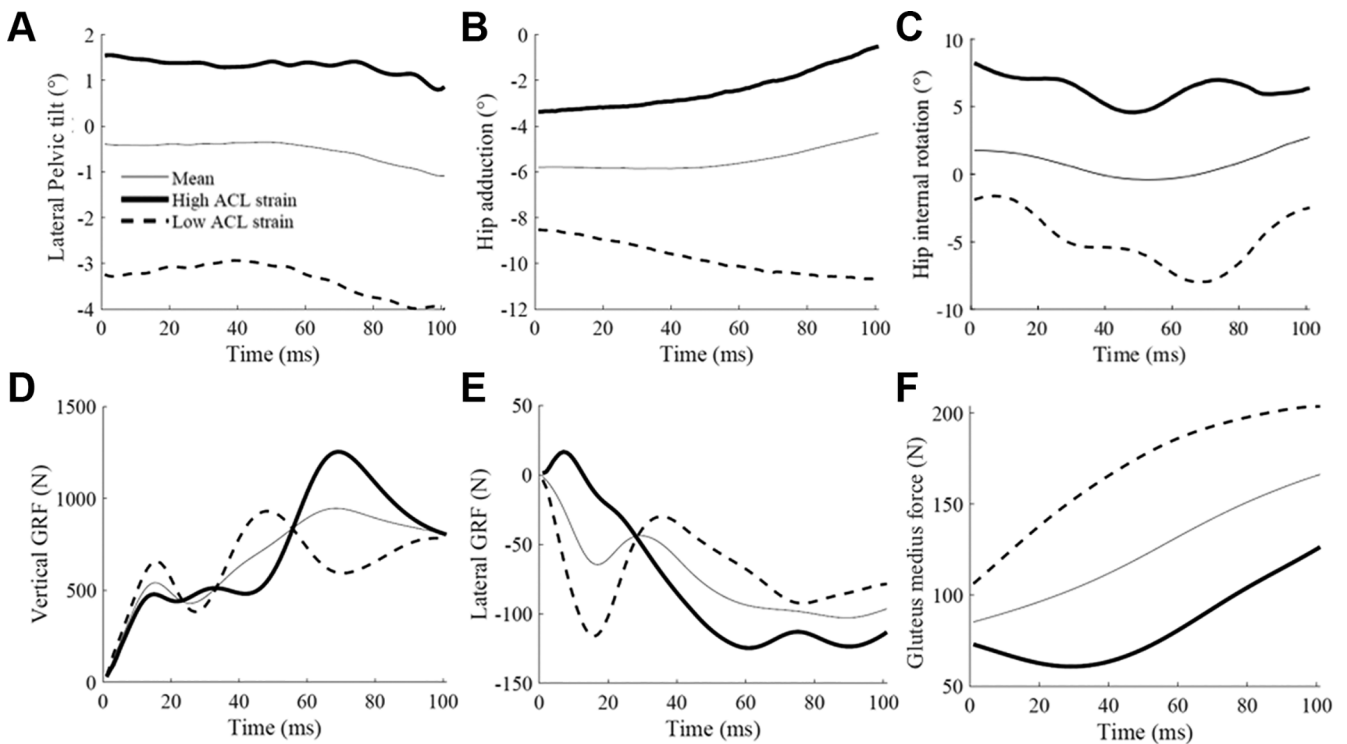


Figure 5. Mean (thin), high ACL strain (thick), and low ACL strain (dashed) waveforms of (A) lateral pelvic tilt, (B) hip adduction, (C) hip internal rotation, (D) vertical ground-reaction force (GRF), (E) lateral GRF, and (F) gluteus medius force (from fiber 2; see Appendix for all 3 fibers) reconstructed from the 4 principal components that significantly predicted high ACL strain trials. Time zero indicates initial contact to the ground. ACL, anterior cruciate ligament.

The ACL strain and force during DVJs seen in the current study were lower compared with previously reported failure loads in young female and male *in vitro* specimens, which were 15% to 30% and 1266 to 2160 N, respectively.^{9,10,52} As expected, the ACL strain and force estimates in this study were substantially lower than measures at failure, as data from laboratory-controlled DVJ trials were used to drive the models. For 15 of the 37 trials, peak strain was observed at IC, when the knee was extended the most. This is consistent with previous fluoroscopic studies.^{12,13} However, the trials that ACL loading was higher than the third quartile presented peak forces at approximately 30 to 60 milliseconds after IC, which is consistent with previously reported ACL failure time from video analysis and cadaveric landing simulations.^{6,30,31,50}

The 6 DOF tibiofemoral joint kinematics revealed that higher knee abduction, internal tibial rotation, and translations toward the anterior, medial, and superior directions were linked to higher ACL strain. The observed increase in tibial translation in the anterior and superior directions indicated that the relative position of the tibial and femoral condyle became more distant in the anteroposterior DOF and closer in proximity in the inferosuperior DOF. This indicated that the femoral condyle rolled posterior and inferior down the tibial plateau. Furthermore, increased knee abduction under a compressive load supported the presence of a continuous compression on the lateral tibial plateau.

With increased internal rotation, the lateral femoral condyle must roll in an inferior and posterior direction at a greater magnitude than the medial femoral condyle to demonstrate these kinematic combinations. These observations indicate that a pivot-shift mechanism occurred, in which the knee abduction created a compression on the lateral plateau of the tibia and induced anterior tibial translation and internal tibial rotation partially because of the posterior tibial slope.³⁵ Specifically, the previous validation study of the model presented that the local angle of the tibial plateau slope, which was calculated on each surface element of the cartilage model, initiated at the tibial eminence and reached its maximal angulation of 22° at the posterior edge of the tibia (see Navacchia et al³⁹). In the trials with high ACL loading, ACL loads were presented even with the increased knee flexion angle in the later phase of landing. This is consistent with previous *in vitro* studies indicating that the ACL is loaded under anterior tibial force and knee abduction moment at the knee flexion angle of 60° to 90°.^{16,33}

The present findings showed that ACL strain was higher during asymmetrical landings, as the waveforms of high ACL strain trials demonstrated higher peak vertical and lateral ground-reaction forces as well as lower gluteus medius force and laterally tilted and shifted pelvic motion. Knee abduction angle during DVJ is a predictor of ACL injury.^{3,25} The present study confirmed that athletes with a high knee abduction angle have higher ACL strain during the DVJ. Note that this study does not prove a single effect of knee abduction angle but rather that other featured biomechanical variables are linked in high ACL strain trials. A recently presented ACL injury reduction program includes

trunk and hip joint exercises to stabilize body control and reduce ACL injury risk.^{22,23,42,48} Although these previous studies could not quantify the effect of such training on ACL loading, the present study supports the results from the training program, suggesting that they have the potential to decrease ACL loading during landing.

Generally, lower muscle forces were observed in high ACL strain waveforms, except for the iliopsoas, vastus intermedius, and gastrocnemius medialis. The vastus intermedius and gastrocnemius medialis might contribute to an increase in ACL loading as antagonists of the ACL.⁴¹ However, a causal analysis was not performed in this study, and the causal effect of these muscles on ACL loading remains unclear.

This study had some limitations. First, the FE analysis was conducted separately from the muscle force estimation step. Since the ligament forces and contact forces on the knee joint resist external joint moments, especially knee abduction/adduction and internal/external rotation moments, there are interactions between ligament forces and muscle forces. As some previous studies have reported,^{20,40} concurrent estimation of muscle, ligament, and joint contact forces would more adequately unveil the causal interaction between these forces. Second, only 1 specimen-specific FE model was used for all the landing trials, and body weight and size were not scaled to each participant.

While the methodology in this study was aimed at simulating ACL loading during an *in vivo* landing with physiologic loading, the results do not represent the participants' actual ACL strain/force during landing. The ACL loads simulated in this study represent the loads in the ligament for a single model landing with various strategies. Patient-specific models that account for personalized anatomy are needed to overcome this limitation. However, *in vivo* patient-specific models with validated ligament properties have not yet been reported in the literature. Promising work has been done to correlate magnetic resonance images with *in vivo* ligamentous material properties³⁸ and may assist in the development of these patient-specific models in future studies. In addition, the validation step of the FE model was performed relative to a knee flexion angle of 25°.³⁹ Therefore, a limitation of the current modeling paradigm is that the results have not been explicitly validated throughout the full range of flexion expressed by each range of motion. Finally, ground-reaction force was applied on the ankle joint center but not on the foot, since the ankle joint was not validated and the movement was kinematically driven.

CONCLUSION

Trials with higher but noninjurious ACL loads were predicted by higher tibial translations toward the anterior, medial, and compressive directions, as well as knee abduction and internal tibial rotation, during DVJ tasks using a musculoskeletal FE model. These findings were observed during an asymmetrical landing in the frontal plane with higher vertical and lateral ground-reaction force, lower gluteus medius force, and laterally tilted and shifted pelvic motion. Clinicians and trainers are encouraged to work with

patients and athletes who present with asymmetrical landing techniques and to utilize preventive training interventions with the goal of encouraging symmetrical landings during practice.

ACKNOWLEDGMENT

The authors acknowledge the support of the staff at the Materials Structural Testing CORE at Mayo Clinic, the Biomechanics Research Lab at Mayo Clinic, and the Sports Health and Performance Institute at The Ohio State University.

REFERENCES

- Ardern CL, Webster KE, Taylor NF, Feller JA. Return to the preinjury level of competitive sport after anterior cruciate ligament reconstruction surgery: two-thirds of patients have not returned by 12 months after surgery. *Am J Sports Med.* 2011;39(3):538-543.
- Bates NA, Mejia Jaramillo MC, Vargas M, et al. External loads associated with anterior cruciate ligament injuries increase the correlation between tibial slope and ligament strain during in vitro simulations of in vivo landings. *Clin Biomech (Bristol, Avon).* 2019;61:84-94.
- Bates NA, Myer GD, Hale RF, Schilaty ND, Hewett TE. Prospective frontal plane angles used to predict ACL strain and identify those at high risk for sports-related ACL injury. *Orthop J Sports Med.* 2020; 8(10):2325967120957646
- Bates NA, Schilaty ND, Krych AJ, Hewett TE. Influence of relative injury risk profiles on anterior cruciate ligament and medial collateral ligament strain during simulated landing leading to a noncontact injury event. *Clin Biomech (Bristol, Avon).* 2019;69:44-51.
- Bates NA, Schilaty ND, Nagelli CV, Krych AJ, Hewett TE. Multiplanar loading of the knee and its influence on anterior cruciate ligament and medial collateral ligament strain during simulated landings and non-contact tears. *Am J Sports Med.* 2019;47(8):1844-1853.
- Bates NA, Schilaty ND, Ueno R, Hewett TE. Timing of strain response of the ACL and MCL relative to impulse delivery during simulated landings leading up to ACL failure. *J Appl Biomech.* Published online April 22, 2020. doi:10.1123/jab.2019-0308
- Boden BP, Dean GS, Feagin JA, Garrett WE. Mechanisms of anterior cruciate ligament injury. *Orthopedics.* 2000;23(6):573-578.
- Boling MC, Bolgla LA, Mattacola CG, Uhl TL, Hosey RG. Outcomes of a weight-bearing rehabilitation program for patients diagnosed with patellofemoral pain syndrome. *Arch Phys Med Rehabil.* 2006;87(11):1428-1435.
- Butler DL, Guan Y, Kay MD, Cummings JF, Feder SM, Levy MS. Location-dependent variations in the material properties of the anterior cruciate ligament. *J Biomech.* 1992;25(5):511-518.
- Chandrashekar N, Mansouri H, Slauterbeck J, Hashemi J. Sex-based differences in the tensile properties of the human anterior cruciate ligament. *J Biomech.* 2006;39(16):2943-2950.
- Cram JR, Kasman GS, Holtz J. *Introduction to Surface Electromyography.* Aspen Publishers; 1998.
- Englander ZA, Baldwin EL, Smith WAR, Garrett WE, Spritzer CE, DeFrate LE. In vivo anterior cruciate ligament deformation during a single-legged jump measured by magnetic resonance imaging and high-speed biplanar radiography. *Am J Sports Med.* 2019;47(13):3166-3172.
- Englander ZA, Garrett WE, Spritzer CE, DeFrate LE. In vivo attachment site to attachment site length and strain of the ACL and its bundles during the full gait cycle measured by MRI and high-speed biplanar radiography. *J Biomech.* 2020;98:109443.
- Fleming BC, Renstrom PA, Beynon BD, et al. The effect of weight-bearing and external loading on anterior cruciate ligament strain. *J Biomech.* 2001;34(2):163-170.
- Ford KR, Myer GD, Schmitt LC, Uhl TL, Hewett TE. Preferential quadriceps activation in female athletes with incremental increases in landing intensity. *J Appl Biomech.* 2011;27(3):215-222.
- Fujie H, Otsubo H, Fukano S, et al. Mechanical functions of the three bundles consisting of the human anterior cruciate ligament. *Knee Surg Sports Traumatol Arthrosc.* 2011;19(suppl_1):47-53.
- Griffin LY, Albohm MJ, Arendt EA, et al. Understanding and preventing noncontact anterior cruciate ligament injuries: a review of the Hunt Valley II meeting, January 2005. *Am J Sports Med.* 2006;34(9):1512-1532.
- Grood ES, Suntay WJ. A joint coordinate system for the clinical description of three-dimensional motions: application to the knee. *J Biomech Eng.* 1983;105(2):136-144.
- Groote FD, Pipeleers G, Jonkers I, et al. A physiology based inverse dynamic analysis of human gait: potential and perspectives. *Comput Methods Biomech Biomed Engin.* 2009;12(5):563-574.
- Halloran JP, Ackermann M, Erdemir A, van den Bogert AJ. Concurrent musculoskeletal dynamics and finite element analysis predicts altered gait patterns to reduce foot tissue loading. *J Biomech.* 2010;43(14):2810-2815.
- Hewett TE, Bates NA. Preventive biomechanics: a paradigm shift with a translational approach to injury prevention. *Am J Sports Med.* 2017; 45(11):2654-2664.
- Hewett TE, Ford KR, Xu YY, Khoury J, Myer GD. Effectiveness of neuromuscular training based on the neuromuscular risk profile. *Am J Sports Med.* 2017;45(9):2142-2147.
- Hewett TE, Ford KR, Xu YY, Khoury J, Myer GD. Utilization of ACL injury biomechanical and neuromuscular risk profile analysis to determine the effectiveness of neuromuscular training. *Am J Sports Med.* 2016;44(12):3146-3151.
- Hewett TE, Myer GD. The mechanistic connection between the trunk, hip, knee, and anterior cruciate ligament injury. *Exerc Sport Sci Rev.* 2011;39(4):161-166.
- Hewett TE, Myer GD, Ford KR, et al. Biomechanical measures of neuromuscular control and valgus loading of the knee predict anterior cruciate ligament injury risk in female athletes: a prospective study. *Am J Sports Med.* 2005;33(4):492-501.
- Hume DR, Navacchia A, Ali AA, Shelburne KB. The interaction of muscle moment arm, knee laxity, and torque in a multi-scale musculoskeletal model of the lower limb. *J Biomech.* 2018;76:173-180.
- Hume DR, Navacchia A, Rullkoetter PJ, Shelburne KB. A lower extremity model for muscle-driven simulation of activity using explicit finite element modeling. *J Biomech.* 2019;84:153-160.
- Jackson DA. Stopping rules in principal components analysis: a comparison of heuristical and statistical approaches. *Ecology.* 1993;74(8):2204-2214.
- Kanamori A, Woo SL, Ma CB, et al. The forces in the anterior cruciate ligament and knee kinematics during a simulated pivot shift test: a human cadaveric study using robotic technology. *Arthroscopy.* 2000; 16(6):633-639.
- Kiapour AM, Quatman CE, Goel VK, Wordeman SC, Hewett TE, Deme-tropoulos CK. Timing sequence of multi-planar knee kinematics revealed by physiologic cadaveric simulation of landing: implications for ACL injury mechanism. *Clin Biomech (Bristol, Avon).* 2014;29(1):75-82.
- Koga H, Nakamae A, Shima Y, et al. Mechanisms for noncontact anterior cruciate ligament injuries: knee joint kinematics in 10 injury situations from female team handball and basketball. *Am J Sports Med.* 2010;38(11):2218-2225.
- Laughlin WA, Weinhandl JT, Kernozek TW, Cobb SC, Keenan KG, O'Connor KM. The effects of single-leg landing technique on ACL loading. *J Biomech.* 2011;44(10):1845-1851.
- Markolf KL, Burchfield DM, Shapiro MM, Shepard MF, Finerman GA, Slauterbeck JL. Combined knee loading states that generate high anterior cruciate ligament forces. *J Orthop Res.* 1995;13(6):930-935.
- Martelli S, Calvetti D, Somersalo E, Viceconti M. Stochastic modelling of muscle recruitment during activity. *Interface Focus.* 2015;5(2):20140094.
- Matsumoto H. Mechanism of the pivot shift. *J Bone Joint Surg Br.* 1990;72(5):816-821.
- Mokhtarzadeh H, Ewing K, Janssen I, Yeow C-H, Brown N, Lee PVS. The effect of leg dominance and landing height on ACL loading among female athletes. *J Biomech.* 2017;60:181-187.

37. Mokhtarzadeh H, Yeow CH, Hong Goh JC, Oetomo D, Malekipour F, Lee PV-S. Contributions of the soleus and gastrocnemius muscles to the anterior cruciate ligament loading during single-leg landing. *J Biomech.* 2013;46(11):1913-1920.

38. Naghibi H, Mazzoli V, Gijbertse K, et al. A noninvasive MRI based approach to estimate the mechanical properties of human knee ligaments. *J Mech Behav Biomed Mater.* 2019;93:43-51.

39. Navacchia A, Bates NA, Schilaty ND, Krych AJ, Hewett TE. Knee abduction and internal rotation moments increase ACL force during landing through the posterior slope of the tibia. *J Orthop Res.* 2019;37(8):1730-1742.

40. Navacchia A, Hume DR, Rullkoetter PJ, Shelburne KB. A computationally efficient strategy to estimate muscle forces in a finite element musculoskeletal model of the lower limb. *J Biomech.* 2019;84:94-102.

41. Navacchia A, Ueno R, Ford KR, DiCesare CA, Myer GD, Hewett TE. EMG-informed musculoskeletal modeling to estimate realistic knee anterior shear force during drop vertical jump in female athletes. *Ann Biomed Eng.* 2019;47(12):2416-2430.

42. Omi Y, Sugimoto D, Kuriyama S, et al. Effect of hip-focused injury prevention training for anterior cruciate ligament injury reduction in female basketball players: a 12-year prospective intervention study. *Am J Sports Med.* 2018;46(4):852-861.

43. Paterno MV, Rauh MJ, Schmitt LC, Ford KR, Hewett TE. Incidence of second ACL injuries 2 years after primary ACL reconstruction and return to sport. *Am J Sports Med.* 2014;42(7):1567-1573.

44. Rajagopal A, Dembia CL, DeMers MS, Delp DD, Hicks JL, Delp SL. Full-body musculoskeletal model for muscle-driven simulation of human gait. *IEEE Trans Biomed Eng.* 2016;63(10):2068-2079.

45. Sartori M, Llyod DG, Farina D. Neural data-driven musculoskeletal modeling for personalized neurorehabilitation technologies. *IEEE Trans Biomed Eng.* 2016;63(5):879-893.

46. Schilaty ND, Bates NA, Krych AJ, Hewett TE. Frontal plane loading characteristics of medial collateral ligament strain concurrent with anterior cruciate ligament failure. *Am J Sports Med.* 2019;47(9):2143-2150.

47. Schilaty ND, Bates NA, Nagelli C, Krych AJ, Hewett TE. Sex-based differences in knee kinematics with anterior cruciate ligament strain on cadaveric impact simulations. *Orthop J Sports Med.* 2018;6(3):2325967118761037.

48. Sugimoto D, Myer GD, Foss KDB, Hewett TE. Specific exercise effects of preventive neuromuscular training intervention on anterior cruciate ligament injury risk reduction in young females: meta-analysis and subgroup analysis. *Br J Sports Med.* 2015;49(5):282-289.

49. Ueno R, Ishida T, Yamanaka M, et al. Quadriceps force and anterior tibial force occur obviously later than vertical ground reaction force: a simulation study. *BMC Musculoskelet Disord.* 2017;18(1):467.

50. Ueno R, Navacchia A, Bates NA, Schilaty ND, Krych AJ, Hewett TE. Analysis of internal knee forces allows for the prediction of rupture events in a clinically relevant model of anterior cruciate ligament injuries. *Orthop J Sports Med.* 2020;8(1):2325967119893758.

51. Ueno R, Navacchia A, DiCesare CA, et al. Knee abduction moment is predicted by lower gluteus medius force and larger vertical and lateral ground reaction forces during drop vertical jump in female athletes. *J Biomech.* 2020;103:109669.

52. Woo SL, Hollis JM, Adams DJ, Lyon RM, Takai S. Tensile properties of the human femur-anterior cruciate ligament-tibia complex: the effects of specimen age and orientation. *Am J Sports Med.* 1991;19(3):217-225.

APPENDIX

Mean (thin line), high ACL strain (thick line), and low ACL strain (dashed line) waveforms of muscle forces reconstructed from the 4 principal components that significantly predicted high ACL strain trials. The numbers for glutei muscles indicate their three fibers in the models. Time zero indicates initial contact to the ground. ACL, anterior cruciate ligament.

